Arch. Metall. Mater. **66** (2021), 3, 709-712

DOI: 10.24425/amm.2021.136366

YUN TAEK KO[1], MIJEONG PARK[2], JINGYEONG PARK[1],
JAEYUN MOON[3], YONG-HO CHOA[1], YOUNG-IN LEE[2*]

MORPHOLOGY CONTROL OF ONE-DIMENSIONAL GALLIUM NITRIDE NANOSTRUCTURES BY MODULATING THE CRYSTALLINITY OF SACRIFICIAL GALLIUM OXIDE TEMPLATES

In this study, we demonstrated a method of controllably synthesizing one-dimensional nanostructures having a dense or a hollow structure using fibrous sacrificial templates with tunable crystallinity. The fibrous Ga_2O_3 templates were prepared by calcining the polymer/gallium precursor nanofiber synthesized by an electrospinning process, and their crystallinity was varied by controlling the calcination temperature from 500°C to 900°C. GaN nanostructures were transformed by nitriding the Ga_2O_3 nanofibers using NH_3 gas. All of the transformed GaN nanostructures maintained a one-dimensional structure well and exhibited a diameter of about 50 nm, but their morphology was clearly distinguished according to the crystallinity of the templates. When the templates having a relatively low crystallinity were used, the transformed GaN showed a hollow nanostructure, and as the crystallinity increased, GaN was converted into a denser nanostructure. This morphological difference can be explained as being caused by the difference in the diffusion rate of Ga depending on the crystallinity of Ga_2O_3 during the conversion from Ga_2O_3 to GaN. It is expected that this technique will make possible the tubular nanostructure synthesis of nitride functional nanomaterials.

Keywords: GaN, Nanofiber, Nanotube, Electrospinning, Chemical Transformation

1. Introduction

Semiconductor nanomaterial has gained considerable attention because of its unique electronic, optical and mechanical properties which make the material superior compare to their bulk forms [1-3]. Gallium nitride (GaN) is one of the most promising compound semiconductor materials among III-nitride family, due to its excellent properties which comprise of wide direct band gap (~3.4 eV), strong stability at high temperature and high voltage circumstances, excellent electron mobility, high physical and chemical stabilities [4-5]. In particular, one-dimensional (1D) GaN nanostructures have received wide attention due to their low dimensionality and precisely controlled geometry which increases the performance of nanometer-scale applications such as optoelectronics, catalysis, sensing, and photovoltaics [6-9]. While several techniques exist for creating 1D GaN nanostructures, electrospinning has emerged as a versatile, scalable, and cost-effective method to synthesize ultra-long nanofibers with controlled diameter and composition [10-12]. In addition, different morphologies and structures can be readily obtained by controlling different processing parameters or subsequent chemical transformation approaches.

Although GaN nanofibers have been synthesized using an electrospinning and post-spinning process including calcination and nitridation, to our knowledge no work has been reported for the synthesis of tubular GaN nanostructures by the process. It is well known that compared with the solid nanofibers, the advantages for the hollow nanofibers include a greater surface area and high aspect ratio which provides more active sites, higher pore volume and surface permeability and shortens the diffusion pathways for ions and electrons [13-15]. In this study, 1D GaN nanostructures were prepared by initial electrospinning, and the subsequent calcination and nitridation. Their morphologies were selectively controlled to nanotubes and nanowires by varying the crystallinity of Ga_2O_3 nanofibers prepared by an electrospinning and a subsequent calcination at different temperatures. The structure and morphology characteristics of samples were investigated by X-ray diffraction, field-emission scanning electron microscopy, and transmission electron microscopy. In addition, the band gap values of the prepared 1D GaN nanostructures were characterized.

[1] HANYANG UNIVERSITY, DEPT. OF ADVANCED MATERIALS SCIENCE AND ENGINEERING, ANSAN 15588, REPUBLIC OF KOREA
[2] SEOUL NATIONAL UNIVERSITY OF SCIENCE AND TECHNOLOGY, DEPT. OF MATERIALS SCIENCE AND ENGINEERING, SEOUL 01811, REPUBLIC OF KOREA
[3] UNIVERSITY OF NEVADA, DEPT. OF MECHANICAL ENGINEERING, LAS VEGAS, 4505 S. MARYLAND PKWY LAS VEGAS, NV 89154, UNITED STATES

* Corresponding author: youngin@seoultech.ac.kr

2. Experimental

Polymer/gallium precursor nanofibers were synthesized by an electrospinning using the solution which was prepared by dissolving 0.5 g of polyvinylpyrrolidone (PVP, Mw: 1,300,000, Sigma-Aldrich) and 1.2787 g of gallium nitrate hydrate ($Ga(NO_3)_3 \cdot xH_2O$, 99.99%, Sigma-Aldrich) in 9 ml of water and ethanol mixture solvent. The precursor solution was transferred into a 10 ml syringe with a stainless-steel nozzle, which was connected to a high voltage power supply. An aluminum foil covered rotating metal collector used as the cathode plate for collecting the nanofibers. It was placed in the front of the needle with a fixed distance of 12 cm between the nozzle tip and collector. A high voltage of 20 kV was applied between them and the spinning rate was controlled at 0.4 mL h^{-1}. The as-spun nanofibers were calcined at 500°C, 700°C and 900°C for 3 h in air to obtain Ga_2O_3 nanofibers with a controlled crystallinity. With regard to the synthesis of GaN nanostructures, the oxide nanofibers were placed in a porcelain boat, and thermally treated at 650°C for 6 h in NH_3 atmosphere using a tube furnace. The oxide samples calcined at 500°C, 700°C and 900°C were denoted G-500, G-700 and G-900, respectively and the samples obtained by nitriding them were designated GN-500, GN-700, and GN-900.

All synthesized nanofibers were analyzed by field-emission scanning electron microscopy (FE-SEM, S-4800, Hitachi, Ibaraki, Japan) to investigate their morphologies and diameters. The average fiber diameter was calculated from the respective SEM images over approx. 200 fibers using software ImageJ (NIH, US). The crystal structure and average crystallite sizes of the nanofibers were characterized by X-ray diffraction (XRD, X'Pert Powder, Malvern Panalytical, Almelo, Netherlands). The microstructures of the nanofibers before and after the chemical transformation step were characterized by transmission electron microscope (TEM, JEM-2100F, JEOL, Tokyo, Japan). Absorption spectra and UV-vis diffuse reflectance spectra were measured using a UV-vis absorption spectrophotometer (UV-vis-2550, Shimadzu Corporation, Japan).

3. Results and discussion

The as-spun polymer/precursor nanofibers must be calcined to remove the polymer and induce crystallization into oxides. At this time, the thermal energy for the calcination acts as a driving force for a nucleation and crystal growth. Therefore, as the input heat energy increases, defects in the crystal are reduced, and grain boundaries are also decreased by grain growth, so that the resulting material has excellent crystallinity. Fig. 1(a) shows the X-ray diffraction patterns of nanofibers calcined at different temperatures, and it can be clearly observed that their crystallinities become excellent as the calcination temperature increases. All diffraction peaks can be indexed to the monoclinic β-Ga_2O_3 phase (JCPDS No. 41-1103). As shown in Fig. 1(b), Ga_2O_3 was completely converted to hexagonal wurtzite GaN (JCPDS No. 65-3410) through the nitridation treatment. Interestingly, the crystallinity of the transformed GaN was different despite the same nitridation conditions. The crystallinity of GaN was highly dependent on the crystallinity of the sacrificial Ga_2O_3 templates, and when the crystallinity of Ga_2O_3 was high, the converted GaN also showed high crystallinity. This difference can be explained as follows. A sacrificial material with good crystallinities is in a more stable state compared to otherwise, and requires a relatively large amount of energy for certain chemical reactions. Therefore, in the transformation process, their atoms are in a high energy state, and a more perfect crystal structure can be formed.

FE-SEM and TEM analysis was carried out to investigate the effect of calcination temperature on the morphology and microstructure of the Ga_2O_3 samples. Fig. 2 shows are the FE-SEM and TEM images of the Ga_2O_3 nanofibers calcined at various temperatures. The average diameters of the G-500, G-700 and G-900 were identified as 70.5 nm, 60.3 nm and 54.7 nm and it can be seen that the diameter decrease as the calcination temperature increases. This change in diameter indicates that the densification and crystal growth of the nanofibers occurred more actively at a relatively high temperature. The TEM images show this difference well. As shown in Fig. 2(d), the G-500 sample has numerous nanoscale crystallites in the individual nanofibers. As the calcination temperature increases, the growth

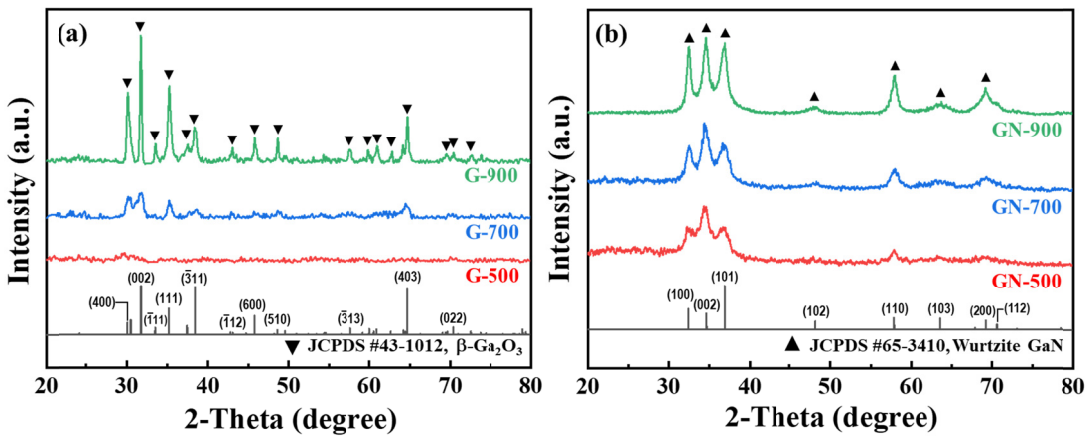

Fig. 1. X-ray diffraction patterns of (a) electrospun nanofibers calcined at different temperature and (b) nanostructures transformed from the nanofibers by a nitridation at 650°C under NH_3 atmosphere

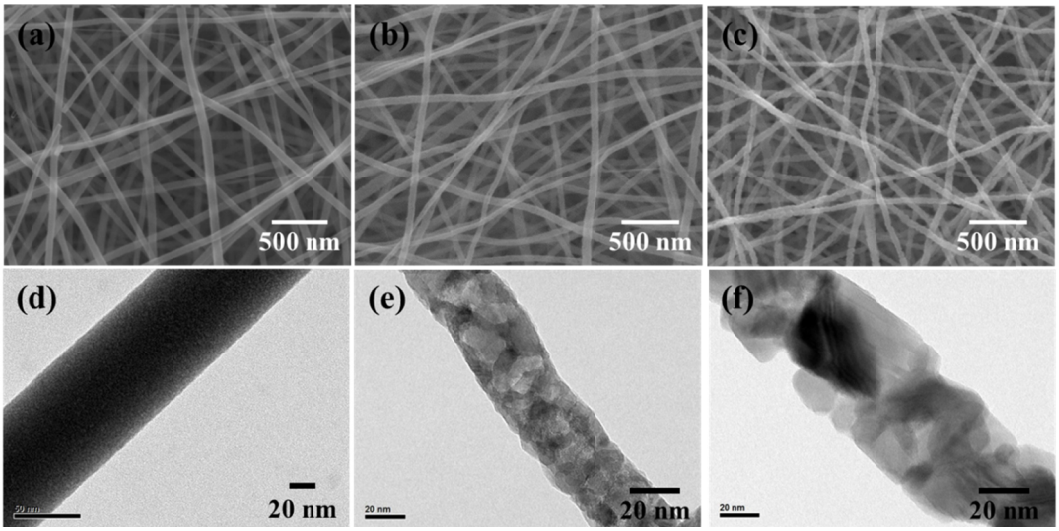

Fig. 2. (a-c) FE-SEM and (d-f) TEM images of (a, d) G-500, (b, e) G-700 and (c, f) G-900

of crystals constituting the nanofibers can be clearly observed from Fig. 2(e, f). These microstructures are in agreement with their XRD patterns.

Fig. 3(a-c) and (d-f) show FE-SEM images and TEM images of the GaN samples transformed from the Ga_2O_3 nanofibers with different crystallinity and microstructure. As shown in Fig. 3, the samples were clearly different in shape even though they were nitrided under the same conditions. The GaN sample (GN-500) which was transformed from the Ga_2O_3 nanofibers (G-500) with the lowest crystallinity, had a diameter and aspect ratio similar to those before transformation, but clearly showed a tubular structure with the wall thickness of about 10 nm. In the case of the GaN sample (GN-700) converted from Ga_2O_3 nanofibers (G-700) showing intermediate level of crystallinity, the nano-sized fibrous structure was well maintained, but unlike GN-500, it showed a solid shape. Finally, GN-900 sample which was transformed from G-900 with the best crystallinity showed a number of partially broken fibers and had the largest grains.

It is a very interesting result that such a difference in crystal size and morphology is clearly observed in the chemically transformed samples under the same conditions. First, it can be seen that the size of crystallites constituting the GaN nanostructures agrees well with the XRD results shown in Fig. 1(b). As the crystallinity of Ga_2O_3 increases, Ga_2O_3 exhibits a more stable state, and a relatively large amount of energy is required to transform it to GaN. Therefore, in the process of conversion, the atoms become a relatively high energy state, and coarse grains are formed through active sintering. Second, the difference between the tubular structure (GN-500) and the solid structure (GN-700) can be explained by the difference in the diffusion rate of Ga in the nitridation process. The low crystallinity of Ga_2O_3 can be regarded as relatively weak bonding between Ga cations and oxygen anions. The cations can rapidly separate the anions and then they can diffuse to the surface for reaction with nitrogen in the early state of the transformation process. Conversely, in the case of Ga_2O_3 with high crystallinity, the separation of

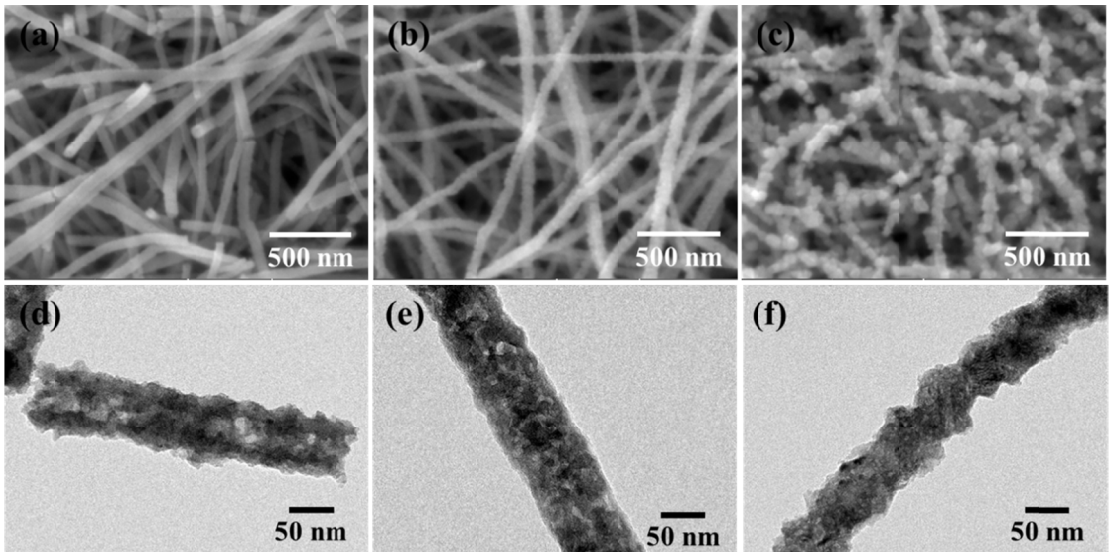

Fig. 3. (a-c) FE-SEM and (d-f) TEM images of (a, d) GN-500, (b, e) GN-700 and (c, f) GN-900

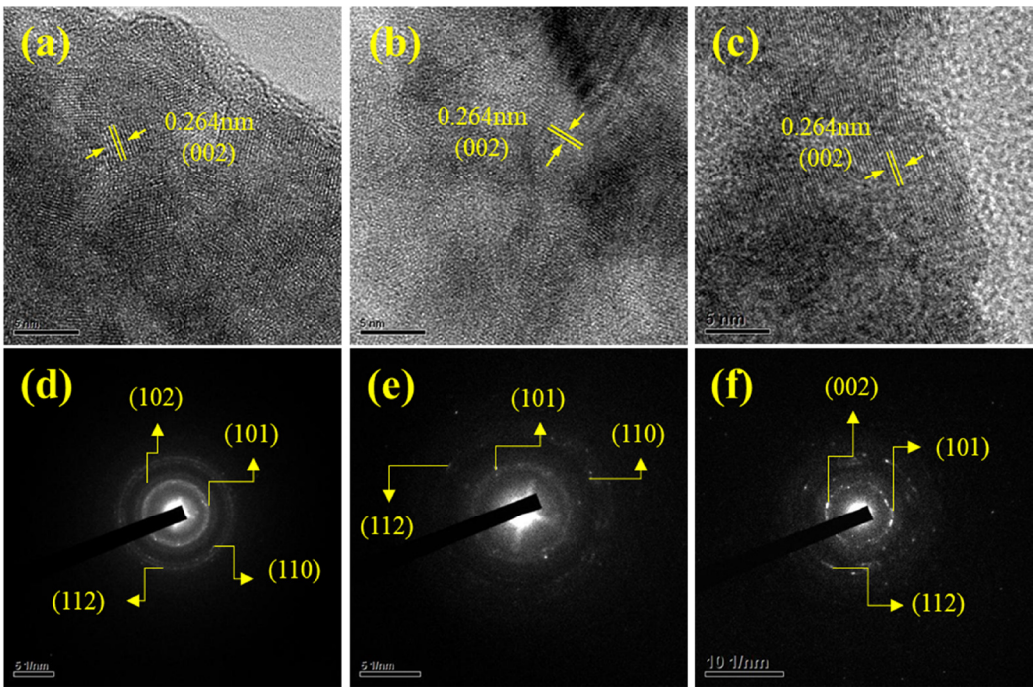

Fig. 4. (a-c) HR-TEM images and (d-f) SAED patterns of the (a,d) GN-500, (b,e) GN-700 and (c,f) GN-900

strongly bound Ga and O may be relatively delayed, and thus the converted GaN exhibits a solid structure because nitrogen can sufficiently diffuse into the sacrificial material to form GaN.

High resolution TEM images and SAED patterns of the transformed GaN nanostructures are shown in Fig. 4. As shown in the images, all nanostructures are structurally poly-crystalline and have a periodic fringe spacing of 0.264 nm, which corresponds to the {002} lattice plane of hexagonal wurtzite GaN. The SAED patterns also show the lattice planes of hexagonal wurtzite GaN. The result was consistent with the results obtained from the XRD analysis and shows a complete transformation from Ga_2O_3 to GaN through the nitridation treatment.

4. Conclusion

In summary, 1D GaN nanostructures with a dense or a hollow structure have been synthesized by chemical transformation of electrospun Ga_2O_3 nanofibers. The synthesized GaN nanostructures are polycrystalline, with a diameter of ~60 nm and high aspect ratio of over 1000. The XRD, FE-SEM and TEM analysis results proved that the morphologies and crystallite sizes of the GaN nanostructures were controlled by tuning the crystallinity of sacrificial Ga_2O_3 templates. When the templates having a relatively low crystallinity were used, the transformed GaN showed a tubular nanostructure, and as the crystallinity increased, GaN was converted into a solid nanostructure. This morphological difference can be explained as being caused by the difference in the diffusion rate of Ga depending on the crystallinity of Ga_2O_3 during the transformation process. It is expected that this technique will make possible the controllable synthesis of tubular or solid 1D nanostructures for various functional nanomaterials.

Acknowledgments

This study was supported by the Research Program funded by the SeoulTech(Seoul National University of Science and Technology).

REFERENCES

[1] X. Yia, P. Yang, Y. Sun, Y. Wu, B. Mayers, B. Gates, Y. Yin, F. Kim, H. Yan, Adv. Mater. **15**, 353 (2003).
[2] L. Cao, J.S. White, J.-S. Park, J.A. Schuller, B.M. Clemens, M.L. Brongersma, Nat. Mater. **8**, 643 (2009).
[3] C.M. Hangarter, Y.-I. Lee, S.C. Hernandez, Y.-H. Choa, N.V. Myung, Angew. Chem. Int. Ed. **49**, 7081 (2010).
[4] W. Han, S. Fan, Q.Q. Li, Y.D. Hu, Science **277**, 1287 (1997).
[5] J.C. Johnson, H.J. Choi, K.P. Knutsen, R.D. Schaller, P. Yang, R.J. Saykally, Nat. Mater. **1**, 106 (2002).
[6] X. Zhang, Q. Liu, B. Liu, W. Yang, J. Li, P. Niu, X. Jiang, J. Mater. Chem. C **5**, 4319 (2017).
[7] H. Wu, Y. Sun, D. Lin, R. Zhang, C. Zhang, W, Pan, Adv. Mater. **21**, 227 (2009).
[8] F. Lu, L. Liu, J. Tian, Appl. Surf. Sci. **497**, 143791 (2019).
[9] S.W. Eaton, A. Fu, A.B. Wong, C.-Z. Ning, P. Yang, Nat. Rev. Mater. **1**, 16028 (2016).
[10] J. Xue, T. Wu, Y. Dai, Y. Xia, Chem. Rev. **119**, 5298 (2019)
[11] G.-D. Lim, J.-H. Yoo, M. Ji, Y.-I. Lee, J. Alloys Compd. **806**, 1060 (2019).
[12] J. Xue, J. Xie, W. Liu, Y. Xia, Acc. Chem. Res. **50**, 1976 (2017).
[13] Y. Sun, B. Mayers, Y. Xia, Adv. Mater. **15**, 641 (2003).
[14] F. Caruso, R. A. Caruso, H. Mohwald, Science **282**, 1111 (1998).
[15] Y.-I. Lee, Mater. Chem. Phys. **180**, 104 (2016).